Runaway Reaction in Solid Explosive Containing a Single Crack due to Gas-Dynamic Choking

Scott I. Jackson and Larry G. Hill

Shock and Detonation Physics, Los Alamos National Laboratory, Los Alamos, NM 87507 USA

Abstract

This work predicts the critical conditions required for the onset of reaction runaway in a narrow high-explosive slot intended to simulate a crack. A model is developed where slot pressurization is attributed to gas-dynamic choking at the slot exit. The combination of the choking and a pressure-dependent reaction rate is shown to be capable of predicting runaway reaction for a range of slot dimensions and pressures, even when the explosive regression is considered. This model agrees with experimental pressure measurements of reaction runaway in slots and provides a mechanism for the erratic burning observed with some explosives under high pressure.

Key words: porosity, deflagration, PBX 9501: fracture, confinement, cookoff
PACS: 82.33.Vx

1 Introduction

Mechanically damaged high explosive (HE) undergoing deflagration has recently [1] been shown capable of generating combustion pressures and flame speeds in excess of those observed in undamaged HE. Flame penetration of HE cracks large enough to support the reaction zone serves to increase the burning surface area and the rate of gas production. Cracks confine the product gas, elevating the local pressure and reducing the reaction zone thickness such that the flame can enter smaller-width cracks. As the reaction zone decreases sufficiently to enter the smallest cracks, the flame surface area will grow appreciably, resulting in rapid pressurization [2] and even deflagration-to-detonation transition [3,4].

Violent reaction, including detonation, has been observed in recent work, however the process is not fully understood. As the explosive burn rate is pressure dependent, it is clear that the confinement of product gas in cracks and pores of HE results in a positive feedback cycle where the burn rate is continually accelerated by increasing local crack pressure. The mechanism of product-gas confinement remains to be determined and has been attributed to processes such as gas-dynamic choking and viscous confinement.

Viscous confinement describes the resistance of the product gas to flow in a crack due to the viscous stresses imposed by the no-slip condition at the crack wall, which induces a pressure gradient over the length of the crack. This confinement mechanism likely becomes more significant as the crack width decreases. The process is further complicated by the fact that the confining surface is also reacting and injecting mass into the flow. The effect of viscosity

is not considered in the current study, although it has been modeled in previous work [5].

The gas-dynamic choking process is less dependent on the crack dimension, requiring only that the product gas generation rate inside the crack exceed the mass flow rate through the crack exit. Choking will occur over a local narrowing of the crack width or for cracks of constant width, at the crack exit.

In reality, both of these processes likely contribute to the runaway reaction mechanism. Detailed simulations of these two confinement effects simultaneously on a single crack can be computationally demanding or even impossible when one considers that, for most real-world applications, a network of cracks will exist (rather than a single one) whose exact extent will be indeterminable. Crack network dimensions will likely have to be estimated stochastically. Detailed analysis is further complicated by the compliance of the explosive/propellant and binder as well as the occurrence of any additional cracks that occur during runaway [5]. As the crack geometry will be statistically determined, any analysis will need to be general enough not to reply on knowledge of an exact network structure.

In this work, we consider gas-dynamic choking as a confinement mechanism for the product gas in a high-aspect-ratio slot in an HE or propellant and predict the conditions required for reaction runaway due to this process. The problem is initially formulated simply and approximately, making it extendable to more complex crack systems. It is then considered in more detail to better understand the limitations of some of the assumptions. Numerical results are also shown to agree with experimental pressure traces [6] from reaction run-

away in a slot in the HMX-based explosive PBX 9501, where a deflagration was observed to rapidly pressurize the slot above 1 kbar in 100 μs. Analysis of the model draws conclusions as to exactly what conditions are erquired for reaction runaway to occur in a confined HE crack due to gas dynamic choking.

2   Slot Pressurization

Consider a two-dimensional gap of width w and of length L located between two deflagrating HE surfaces (Fig. 1). The gap is bounded on one side by a wall and open on the other side to a reservoir of significantly larger volume than the gap, such that the reservoir pressure will change very slowly relative to the gap pressure P once choking occurs.

We assume the flame rapidly spreads throughout the slot before it has a chance to pressurize appreciably. Thus, initially all HE surfaces of the slot are ignited and the slot pressure is equal to the reservoir pressure. The product gases from the burning walls are injected into the slot from the reacting HE and escape from the open end.

The problem is now analyzed in two stages. Initially, the regression rate of the reacting HE slot walls is neglected and gas dynamic choking is assumed to immediately occur at the slot exit. This allows the unsteady mass equation to be analytically integrated for the pressure in the control volume over time. The second stage of analysis models the regression of the HE walls numerically and allows the slot to blowdown isentropically prior to the onset of choking.

2.1 Fixed Control Volume with Immediate Choking

Applying the unsteady mass equation to the fixed control volume in Fig. 1 yields

$$\frac{\mathrm{d}\rho}{\mathrm{d}t} = \frac{2\rho_{in}u_{in}}{w} - \frac{\rho_{out}u_{out}}{L} . \tag{1}$$

The greatest mass flux out of the slot occurs when the flow is choked. Assuming isentropic choked flow of a perfect gas at the slot exit, Eq. 1 becomes

$$\frac{\mathrm{d}\rho}{\mathrm{d}t} = \frac{2\rho_{in}u_{in}}{w} - \frac{\rho}{L}\left(\frac{\gamma+1}{2}\right)^{\frac{1}{1-\gamma}}\left(\frac{2\gamma\,RT}{\gamma+1}\right)^{\frac{1}{2}} \tag{2}$$

where the gas properties over the length of the slot are assumed to average to the stagnation condition and carry no subscripts.

Evaluation of the middle term of Eq. 2 at the burning burning surface allows $\rho_{in}u_{in} = \rho_e u_e$, where u_e is the HE regression rate and ρ_e is the HE initial density. As stated previously, movement of the control volume is neglected. This is mathematically equivalent to assuming that the reservoir gas density ρ is much less than ρ_e, a valid approximation for lower slot pressures. This is also valid if the runaway process occurs rapidly relative to regression of the HE surface.

Maienschein and Chandler [7] have found the burn rate of PBX 9501 to be well approximated between 200 and 4000 bar by

$$u_e = c + bP \tag{3}$$

where $b = 9.5 \times 10^{-10}$, $c = 3.4 \times 10^{-3}$, P is in Pa, and u_e is in m/s. Thus $\rho_e u_e$ can be substituted for $\rho_{in}u_{in}$ in Eq. 2, allowing the mass inflow per unit

area to the slot to be expressed as a function of the pressure in the slot and the initial density of the explosive.

For high-aspect-ratio slot geometries, the reaction zone volume is comparable to the slot volume, and the slot temperature T can be approximated as constant at the reaction zone temperature, allowing Eq. 2 to be rewritten as

$$\frac{\mathrm{d}P}{\mathrm{d}t} = \frac{2\rho_e\, RT}{w}\,(c + bP) - \frac{RT}{L}aP \tag{4}$$

where

$$a = \left(\frac{\gamma + 1}{2}\right)^{\frac{1}{1-\gamma}} \left(\frac{2\gamma}{(\gamma + 1)\,RT}\right)^{\frac{1}{2}}. \tag{5}$$

This result can then be integrated with the initial condition $P(t = 0) = P_0$ to yield,

$$P\,(t) = \left(P_0 + \frac{d}{e}\right)\exp\,(e\,t) - \frac{d}{e} \tag{6}$$

where

$$d = \frac{2\rho_e\, RT}{w}c \tag{7}$$

and

$$e = \frac{2\rho_e\, RT}{w}b - \frac{RT}{L}a \tag{8}$$

such that for a given explosive and initial conditions, the solution for slot pressure P is a function of time t only.

For Eq. 6 with fixed explosive properties and initial pressure, different solution behaviors are observed when varying the slot aspect ratio L/w as shown in

6

Fig. 2. For low aspect ratios, such as the $w = 1.52$ ($L/w = 125$), the slot pressure asymptotes to a steady value as time progresses. As the aspect ratio is increased, the pressure asymptote increases as shown with the $w = 1.09$ ($L/w = 174$) case. At a certain aspect ratio, however, the pressure does not asymptote but instead rapidly rises to infinity, as shown for $w = 1.52$ ($L/w = 243$).

This rapid pressurization in high-aspect-ratio slots can only occur when the flow of gas into the slot always exceeds the outflow rate. A curve for when the outflow rate is equal to the inflow rate can be found by setting the mass storage variable dP/dt from Eq. 4 to zero and solving for L/w,

$$\frac{L}{w} = \frac{1}{2} \frac{aP}{\rho_e \left(c + bP \right)} \; . \tag{9}$$

This is the steady-state solution for the choked slot with mass inflow from the walls.

Equation 9 is shown in Fig. 3 along with vector arrows to indicate the sign and relative magnitude of Eq. 4 at each position off of the steady-state solution. Two distinct regimes are identified. For a range of L/w, a balance between the inflow and outflow rates exists as described by Eq. 9 ("steady solution" in Fig. 3). The vectors show that all solutions in this steady-choking regime move towards Eq. 9 as time progresses. The upper limit of this steady choking regime is bounded by an asymptote described by

$$\frac{L}{w} = \frac{a}{2\rho_e b} \; . \tag{10}$$

For values of L/w above this asymptote, no positive steady-state choking solution exists and the pressure continuously increases with time as indicated

7

by Eq. 4. The region is considered the runaway-reaction regime as the pressurization has no upper limit.

2.2 Moving Control Volume with Variable Exit Condition

Modeling the regression rate of the HE walls introduces an additional term into the unsteady mass equation due to the increasing storage volume

$$\frac{\mathrm{d}\rho}{\mathrm{d}t} + \frac{\rho}{w}\frac{\mathrm{d}w}{\mathrm{d}t} = \frac{2\rho_{in}u_{in}}{w} - \frac{\rho_{out}u_{out}}{L} \ . \tag{11}$$

Assuming a perfect gas and the pressure-dependent regression rate [7] yields the following differential equation

$$\frac{\mathrm{d}P}{\mathrm{d}t} = \frac{2\rho_e RT}{w}u_e - \frac{RT}{L}\rho_{out}u_{out} - \frac{2}{w}Pu_e \tag{12}$$

where

$$\frac{\mathrm{d}w}{\mathrm{d}t} = 2u_e = 2\left(c + bP\right) \tag{13}$$

from Eq. 3. As before, the temperature T is approximated as constant at the reaction zone temperature.

For this case, we will assume isentropic flow expansion from the control volume exit to the reservoir pressure when

$$\frac{P}{P_r} < \left(\frac{\gamma+1}{2}\right)^{\frac{\gamma}{\gamma-1}} \tag{14}$$

where P_r is the reservoir pressure outside the slot. For $\gamma = 1.3$, the critical ratio $P/P_r \approx 1.83$. For ratios below this condition,

$$\rho_{out} u_{out} = P M_{out} \left(\frac{\gamma}{RT}\right)^{\frac{1}{2}} \left(1 + \frac{\gamma - 1}{2} M_{out}^2\right)^{\frac{1+\gamma}{2(1-\gamma)}} \tag{15}$$

where M_{out} is the Mach number of the exit flow and

$$M_{out} = \left(\frac{2}{\gamma - 1}\left[\left(\frac{P}{P_r}\right)^{\frac{\gamma-1}{\gamma}} - 1\right]\right)^{\frac{1}{2}}. \tag{16}$$

Once Eq. 14 is violated, choking occurs at the gap exit. For this condition, the flow at the slot exit is sonic and the choked flow relations can be used to determine the mass flux

$$\rho_{out} u_{out} = \frac{P}{RT}\left(\frac{\gamma + 1}{2}\right)^{\frac{1}{1-\gamma}} \left(\frac{2\gamma RT}{\gamma + 1}\right)^{\frac{1}{2}} \tag{17}$$

as in the previous section. If only choked flow is considered, Eq. 12 with Eq. 17 is analytically integrable. However, we numerically integrate Eq. 12 (with Eq. 15 or 17 as appropriate) along with Eq. 13 when monitoring for the onset of choking and unchoking, which can occur as slot width increases. For finite reservoir volumes, tracking the mass flux into the reservoir can also identify when P_r increases sufficiently to terminate choking.

When compared to the fixed control volume solution for the previous section, solutions to Eq. 12 pressurize to very high pressures for high-aspect-ratio slots, but do not proceed to infinity. The regime map best illustrates possible solutions by setting $\mathrm{d}P/\mathrm{d}t = 0$ in Eq. 12, which along with Eq. 17, again yields a steady state solution that can be solved for L/w

$$\frac{L}{w} = \frac{RTaP}{2\left(c + bP\right)\left(\rho_e RT - P\right)}. \tag{18}$$

9

This curve is plotted along with vectors from Eq. 12 with Eq. 17 in Fig. 4. For low aspect ratios, the steady solution is similar to the previous case, but for increased pressures it rolls over to an asymptote at $\rho_e = P/RT$. This is a result of the inclusion of the perfect gas equation of state: The density of the product gases cannot exceed that of the solid explosive. Thus the maximum slot pressure that can be achieved with this equation of state is $P = \rho_e RT$, which for typical values of explosive density, product gas temperature, and gas constants is on the order of 10 kbar. These large pressures can still be considered infinite from an engineering perspective in that most assemblies are not built to withstand such loading. All solution trajectories proceed from right to left in Fig. 4 as slot wall regression (which is not represented by the vectors) decreases the aspect ratio over time.

3 Comparison with Experiment

Figure 5 shows experimental data [6] of reaction runaway in PBX 9501 containing a single slot of width $w = 80$ μm, length $L = 19$ cm, and depth $d = 1.27$ cm that exhausted into a 10.23 cc reservoir volume. Curves from the fixed and moving wall models (Eq. 6 and Eq. 12) are shown next to each experimental pressure trace measured in the slot. Representative properties of PBX 9501 and its combustion products were used to calculate the model curves and they have been offset in time only to fit each experimental trace. For the experiment, the first half of the slot was filled with propellant in order to rapidly pressurize the slot, creating a choking condition and pressurizing the reservoir to $P_0 \approx 20$ bar. Transducer P1 was not modeled as it was located outside the open end of the slot in the reservoir volume. Transducer P4 was at

10

the closed end of the slot. Transducers P2 and P3 were located 7.0 cm and 13.0 cm inside the slot, respectively. The experimental test cell failed mechanically during the test when pressures reached 1 kbar, resulting in a decrease in the measured pressure. The fixed control volume model agrees well with the experimental data and provides evidence that pressurization of the slot is indeed due to the onset of gas-dynamic choking. The lower rate of increase associated with the moving wall control volume provides even better agreement with the experimental data. The expected trajectory of the experimental data, modeled with the moving control volume model, is plotted in Fig. 4 as a function of slot pressure versus aspect ratio. The curve starts at $L/w = 2375$ and P_0 $= 20$ bar and smoothly increases to 7 kbar before the widening of the gap causes the pressure to decrease to approximately 1.5 kbar. At this point, the choking criterion fails due to pressurization of the reservoir (with an assumed perfect gas reservoir at 500 K); the slot and reservoir pressure is equal from that point on.

Comparison of this analysis to experiments [6] is of limited value due to the suspected failure of the gasket material used in the tests. For the experiments, two slot lengths, 4.1 and 19.0 cm were used and the slot width was kept constant at 80 μm. This corresponds to L/w ratios of 508 and 2375, both well into the runaway reaction regime shown in Fig. 3, however, runaway reaction was never observed in the 4.1-cm-long-tests and was only observed in half of the 19.0-cm-long tests. Postshot disassembly revealed that gasket failure consistently occurred in cells that did not run away, allowing gas to vent from other portions of the slot besides the exit. This leakage is thought to have driven the solution to the left in Figs. 3 and 4, resulting in lower pressures than expected. Nevertheless, runaway reaction did occur in half of the long

11

slot tests. Presumably in these tests, the gasket did not fail until after the cell was destroyed by the large pressures generated. Experimental work currently underway attempts to minimize the potential for depressurization due to gasket failure and should allow better exploration of the pressure runaway relationship.

4   Flame Entry Implications

Belyaev proposed a relation to predict the minimum pressure at which a flame will exist in a slot by assuming that product gas inflow heats the slot walls until Zeldovich's ignition criteria are met [8].

$$P^{1+2n}w^2 = const \tag{19}$$

Subsequent work [9] has determined that, for PBX 9501, $n = 0.92$ and $const = 8 \times 10^8$ kg^{3}m^{-1}s^{-6}. Belyaev's relation is shown in Fig. 6 for $L = 500$ μm (corresponding to $w = 4$ μm at $L/w = 125$ and $w = 1.4$ μm at $L/w = 350$) representing a common crack width observed in thermally damaged PBX 9501 [10]. Steady burning cannot occur for pressures below Belyaev's line in Fig. 6. For values of L/w where the steady-choking solution lies below Belyaev's line, flames will be driven to extinction. For larger values of L/w, continuous burning modes are available above Belyaev's line in both the runaway-reaction regime and part of the steady-choking regime. The end effect is that, for very small, high-aspect-ratio cracks, sustained flame intrusion does not occur until the pressure is sufficiently high for continuous burning to occur. Then the reaction quickly runs away or is driven to high steady-choking pressures capable of causing mechanical failure of the HE and most casing materials. This

sudden flame intrusion followed by rapid pressurization may contribute to the "erratic burning" observed at elevated pressures [7].

5   Assumptions and Future Work

These models are primarily intended to demonstrate the potential for gas-dynamic effects to drive runaway reaction. As such, many simplifications have been made to facilitate presentation of the model. In most geometries, the neglected material compressibility will act to decrease L/w as burning progresses, limiting runaway. That said, inertial confinement will have the reverse effect during rapid pressurizationn. Accounting for control volume movement due to HE surface regression with a perfect gas equation of state results in a high pressure limit, above which runaway does not occur. The improbability of a calorically perfect, ideal gas with a constant, pressure-independent reaction zone temperature is also acknowledged, as is the existence of a homogenous, subsonic, constant-pressure slot reservoir state. For early times, one-dimensional wave motion is a more probable mode of information propagation and is hinted at in experimental work [6]. The effect of viscosity is worthy of further consideration with this model, as is extension of these concepts to a connected network of porosity. These are considered in ongoing work.

6   Conclusions

Models have been developed where runaway reaction in high explosive containing a narrow slot (simulating a crack) was attributed to gas-dynamic choking

13

causing mass accumulation in the slot. The combination of choking and a pressure-dependent reaction rate was shown to be capable of predicting the pressure increase in the slot between two pieces of PBX 9501 explosive. The models were used to identify crack dimensions and pressure ranges where runaway reaction is likely to occur. As the basic runaway model depends only on crack surface area, volume, and outflow area, it is extendable to statistically determined crack networks. When combined with Belyaev's relation, the models imply that, for extremely small cracks, the only stable burning modes available will rapidly run away to very high pressures.

7   Acknowledgments

References

[1] H. Berghout, S. Son, C. Skidmore, D. Idar, B. Asay, Combustion of damaged PBX 9501 explosive, Thermochimica Acta 384 (2002) 261–277.

[2] L. Hill, Burning crack networks and combustion bootstraping in cookoff explosions, in: Shock Compression of Condensed Matter, American Physical Society, 2005, pp. 531–534.

[3] B. Kondrikov, A. Karnov, Transition from combustion to detonation in charges with a longitudinal cylindrical channel, Combustion, Explosion, and Shock Waves 28 (3) (1992) 263–269.

[4] P. Dickson, B. Asay, B. Henson, L. Smilowitz, Thermal cook-off response of confined PBX 9501, The Royal Society 460 (2004) 3447–3455.

[5] Y. Lu, K. Kuo, Modeling and numerical simulation of combustion process inside a solid-propellant crack, Propellants, Explosives, Pyrotechnics 19 (1994) 217–226.

[6] S. Jackson, L. Hill, H. Berghout, S. Son, B. Asay, Runaway reaction in a solid explosive containing a single crack, in: 13th International Detonation Symposium, Office of Naval Research, 2006, pp. 646–655.

[7] J. Maienschein, J. Chandler, Burn rates of pristine and degraded explosives at elevated temperatures and pressures, in: 11th International Symposium on Detonations, Office of Naval Research, 1998, pp. 872–879.

[8] H. Bradley, T. Boggs, Convective burning in propellant defects: A literature review, Tech. Rep. NWC-TP-6007, Naval Weapons Center, China Lake, CA (1987).

[9] H. Berghout, S. Son, L. Hill, B. Asay, Flame spread though cracks of pbx 9501 (a composite oxtahydro-1,3,5,7-tetranitro-1,3,5,7-tetrazocine-based explosive), Journal of Applied Physics 99 (2006) 114901.

[10] G. Parker, P. Peterson, B. Asay, P. Dickson, W. Perry, B. Henson, L. Smilowitz, M. Oldenborg, Examination of morphological changes that affect gas permeation through thermally damaged explosives, Propellants, Explosives, Pyrotechnics 29 (2004) 274–281.

8 Figures

9 Figure Captions

Figure 1: A sketch of the control volume (dashed line) for a two-dimensional slot.
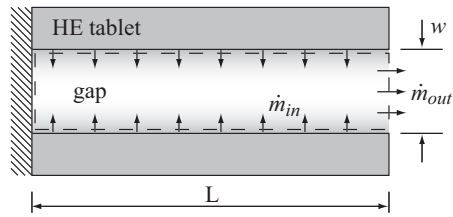
Fig. 1.
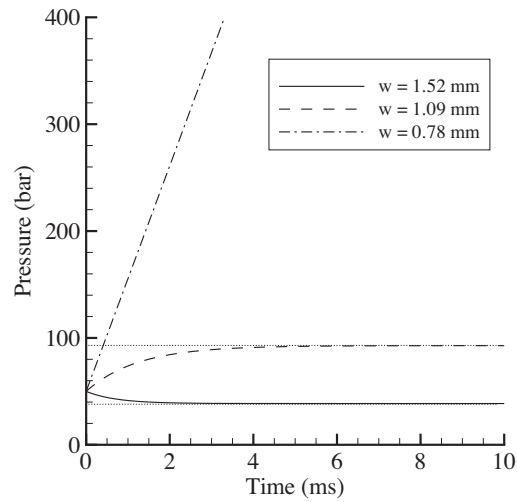
Fig. 2.
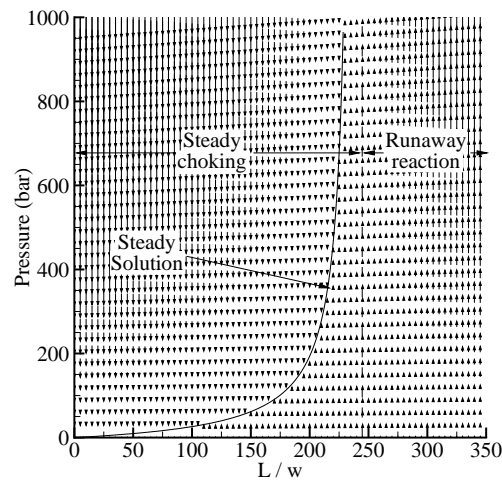
Fig. 3.

Figure 2: Slot pressure versus time for three different width slots. All have the same length $L = 19$ cm. Dotted lines are asymptotes.

16
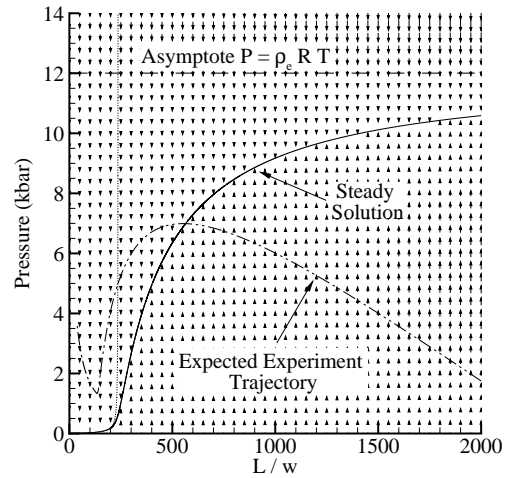
Fig. 4.
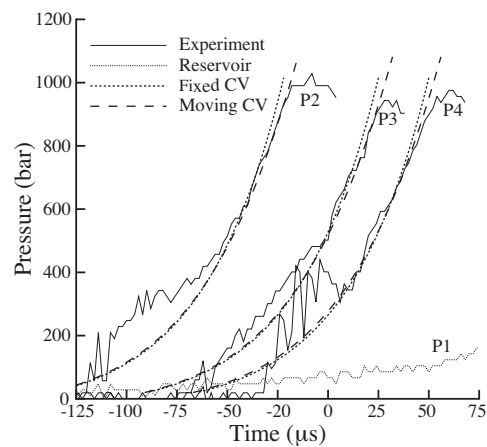
Fig. 5.

Figure 3: A plot illustrating the regimes of slot pressurization. PBX 9501 parameters used are listed in Fig. 5.

Figure 4: Regimes map for a slot with wall regression. The steady solution for the slot with fixed walls (dotted line) is shown for comparison. PBX 9501 parameters same as in Fig. 5.

Figure 5: Reaction runaway in a narrow slot. Equation 6 fit to experimental traces of pressure runaway from Jackson et al. [6]. Timebases for curves from

17
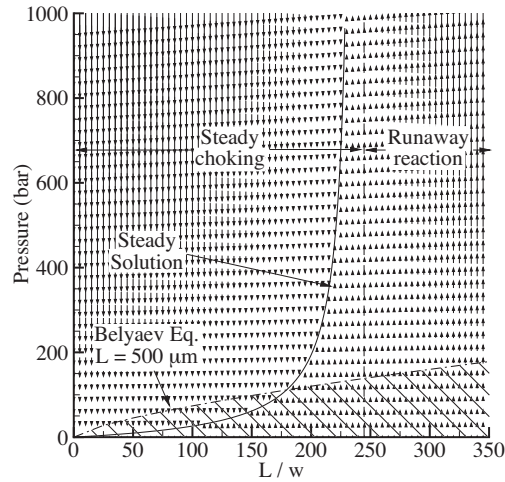
Fig. 6.

Eq. 6 are offset in time by -137, -90, and -65 μs. Traces are clipped after cell failure for clarity. Parameters used for calculations were characteristic of PBX 9501 properties: $\gamma = 1.3$, $\rho_e = 1830$ kg/m^3, $R = 243$ m^2/(s^2 · K), and $T = 2700$ K.

Figure 6: The fixed control volume regime map with constraints imposed by choking onset considerations and Belyaev's equation for a slot with L = 500 μm. PBX 9501 parameters same as in Fig. 5.